

# Efficient Federated Finetuning of Tiny Transformers with Resource-Constrained Devices

Kilian Pfeiffer<sup>1</sup>, Mohamed Aboelenien Ahmed<sup>1</sup>, Ramin Khalili<sup>2</sup>, Jörg Henkel<sup>1</sup>

<sup>1</sup>Karlsruhe Institute of Technology Karlsruhe, Germany

<sup>2</sup>Huawei Research Center, Munich, Germany

kilian.pfeiffer@kit.edu, mohamed.ahmed3@kit.edu, ramin.khalili@huawei.com, henkel@kit.edu

## Abstract

In recent years, Large Language Models (LLMs) through Transformer structures have dominated many machine learning tasks, especially text processing. However, these models require massive amounts of data for training and induce high resource requirements, particularly in terms of the large number of Floating Point Operations (FLOPs) and the high amounts of memory needed. To fine-tune such a model in a parameter-efficient way, techniques like Adapter or LoRA have been developed. However, we observe that the application of LoRA, when used in federated learning (FL), while still being parameter-efficient, is memory and FLOP inefficient. Based on that observation, we develop a novel layer finetuning scheme that allows devices in cross-device FL to make use of pretrained neural networks (NNs) while adhering to given resource constraints. We show that our presented scheme outperforms the current state of the art when dealing with homogeneous or heterogeneous computation and memory constraints and is on par with LoRA regarding limited communication, thereby achieving significantly higher accuracies in FL training.

## 1 Introduction

In recent years, Large Language Models (LLMs) have dominated various machine learning tasks, particularly next token prediction and text classification, while Vision Transformers (ViTs) have closed the gap with convolutional neural networks (CNNs) in vision tasks. However, these models require massive amounts of data (e.g., huge quantities of text for LLMs) and are very power-hungry for training, as they have billions of parameters to adjust [1]. As these LLMs, like GPT2 [2] or LLaMA [3], have billions of parameters and are trained on large quantities of text, they generalize well to many downstream tasks in the text domain. Similarly, in vision, multimodal Transformers can generalize well to detecting objects in an image [4, 5].

In many downstream applications, e.g., in next-word prediction or object classification on smartphones or internet of things (IoT) devices, deploying such large models imposes high resource requirements for inference, potentially causing high latency and high energy consumption. Although, through generalization, they can achieve the desired accuracy, for many tasks, they are not necessarily required, as tiny specialized models would suffice. In particular, we observe that tiny models that require  $\sim 60 \times$

fewer resources (Floating Point Operations (FLOPs)) for inference compared to a lightweight GPT-2 124M model can perform similarly<sup>1</sup> in next-token prediction tasks (refer to fig. 1). However, these specialized models require a sufficient amount of problem-specific data to serve as a replacement. In many cases, this problem-specific data resides on *resource-constrained* edge devices (such as smartphones or IoT devices), is privacy-sensitive, and cannot be centrally stored and processed. While in centralized training, several hundred-watt server GPUs are available, edge devices are very limited in their resources and can only spend a few watts on training. Additionally, such devices can have *heterogeneous* capabilities [6].

To make use of the devices' data, training must be performed on the devices themselves. In recent years, federated learning (FL) has emerged as a privacy-sensitive alternative to centralized training and has shown success in many domains such as smartphone applications, healthcare, and robotics [7, 8, 9, 10]. In this work, we study how tiny pretrained Transformer models can be adapted to downstream tasks using FL with heterogeneous resource-constrained devices.

To adapt large models to downstream tasks, recently, popular techniques like Adapter [11] and LoRA [12] have been introduced, mainly allowing the adaptation of such models in a parameter-efficient way. However, we observe that while being parameter-efficient, techniques like LoRA still require massive amounts of memory for training in the case of tiny models. The reason for this is that LoRA mainly reduces the memory overhead of gradients and optimizer states but does not lower the activation memory. For large models, this typically suffices as the weights and gradients account for most of the required training memory. We observe that the memory footprint of tiny language models and ViTs is mainly dominated by the activation memory (appendix A).

We compare LoRA against finetuning individual layers of a set of tiny neural networks (NNs) (Transformers with 3–12 layers, 3 heads, and an embedding size of 92) that were pretrained on OpenWebText [14] and trained in a federated manner to perform next-token prediction on Shakespeare [13] from the Leaf benchmark. From fig. 1, we can

<sup>1</sup>Parts of the test set may be in GPT's training set, hence increasing accuracy.

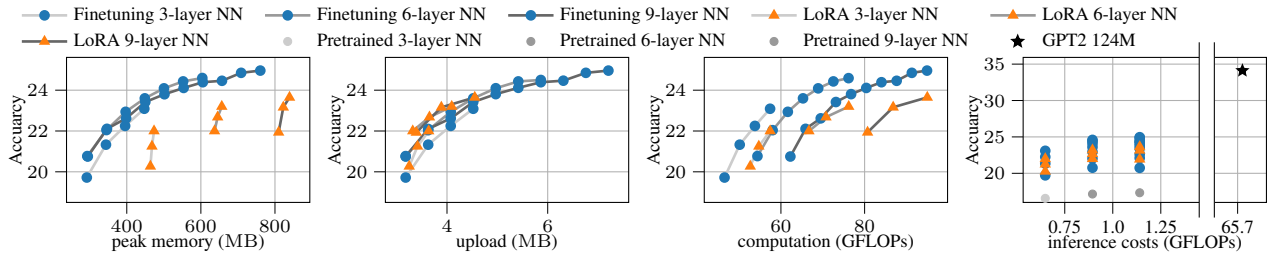


Figure 1: Comparison of downstream performance and resource requirements for next-token prediction on Shakespeare [13] using layer finetuning (with layers frozen from first to last, where each dot represents a specific number of layers being frozen) and LoRA with tiny Transformers pretrained on OpenWebText, having 3, 6, and 9 layers. We observe that while LoRA (with ranks 24, 12, 3) can achieve gains in communication efficiency, it requires significantly more peak memory and FLOPs to reach the same accuracy. Hyperparameters and details are provided in section 4.1. GPT2 is included to highlight inference costs (accuracy is based on GPT2’s tokenizer and test data may be part of GPT2’s training set).

draw the following conclusion: For tiny language models, LoRA can achieve similar communication savings compared to layer finetuning. With LoRA, only the low-rank adapters need to be uploaded, while with layer finetuning, only the trained layers need to be uploaded. However, besides memory, we observe that compared to layer finetuning, LoRA requires significantly more computation (as backpropagation is needed from the last to the first layer). Motivated by that observation, we re-evaluate existing FL strategies that address resource constraints and heterogeneous devices in cross-device FL.

Different from the state of the art, we assume that the FL models are already pretrained. Furthermore, we assume that we have a selection of differently sized NNs to choose from. We observe that when using pretrained NNs, layer finetuning outperforms LoRA-derived techniques [15] as well as existing state-of-the-art methods [16, 17, 18, 19, 20]. Based on our observations, we propose a strategy that, through NN selection and layer finetuning, allows reaching the highest accuracy while adhering to a given device constraint. In summary, we make the following novel contributions:

- We are the first to study resource-constrained cross-device FL with the availability of pretrained models. We rigorously evaluate existing FL strategies and observe that layer finetuning outperforms vanilla LoRA [12] as well as recent FL adaptations for heterogeneity [15]. Furthermore, with pretrained tiny NN models, layer finetuning also surpasses existing FL techniques [18, 17, 19, 16, 20]. Specifically, we study FL downstream tasks such as Shakespeare, CIFAR10, and CIFAR100.
- Existing works assume a fixed NN that must be trained while adhering to device constraints. In this work, we assume a set of pretrained NN architectures is available for selection. Based on our observations, we propose Constraint-Aware Federated Finetuning (CAFF), an architecture selection technique that achieves the highest accuracy given a device constraint.
- We evaluate the performance of state-of-the-art techniques and CAFF in heterogeneous settings. Additionally, our technique promotes greater fairness for weaker devices.

## 2 Related Work

**Subset-based training:** Resource constraints, and especially heterogeneous devices in FL, are tackled in a variety of works. A large branch of works applies *submodel* training [21, 19, 18, 17]. Caldas *et al.* [13] were among the first to propose such a scheme. Specifically, they randomly drop filters in CNNs to create a submodel with lower resource intensity. Both schemes in HeteroFL [18] and FjORD [19] hierarchically drop filters, such that devices with specific constraints always receive the same parameters. Additionally, in FjORD, each device alternates between subsets that are within its capabilities. However, both require that the most capable device is able to train the full NN model. FedRolex [17] addresses this issue by applying a rolling-window scheme over the parameter set, such that eventually all parameters receive training. Lastly, DepthFL [20] trains subsets by splitting the NN depthwise, using early exits for constrained devices in combination with self-distillation. Beyond training of subsets, freezing and quantization have been considered to address the heterogeneity challenges.

**Freezing in FL:** In CoCoFL [22], freezing and quantization are used to lower the resources in heterogeneous training. However, it is assumed that the NN model is trained from scratch, i.e., there has to be a set of devices capable of training the first layers. Hence, the selection technique aims to propagate the gradients as far back as possible within the NN structure. Freezing has also been used to progressively increase the size of the NN and thereby save resources. Wang *et al.* propose ProgFed [23], where the NN is progressively increased by stacking layers on top of each other. Each time a new layer is stacked on the previously trained NN, the NN’s head is removed and replaced. The authors show that this enables a significant reduction in required data upload and computations. However, eventually devices have to train the fully stacked NN as no freezing is applied, thereby requiring memory capabilities for fully training the NN model. This constraint is loosened by Successive Layer Training [24], where a model is progressively built up, but more and more early layers get frozen; thereby, the technique allows to obey to a given memory constraint. However, both techniques assume training a model in a federated

fashion from scratch and do not consider pretrained models. Freezing in FL has also been used to tackle other problems, like personalization [25]. Lastly, freezing schemes have been proposed to tackle communication efficiency [26].

**Low-rank factorization:** Low-rank factorization has been considered in tackling heterogeneity [16, 27] in FL. Similar to LoRA [12], low-rank adapters are used, i.e., a layer that maps from the input space to a lower-rank space and a second layer that maps from the lower-rank space to the output space. Differently from LoRA, these techniques replace the NN’s main parameters using a lower-rank approximation gathered through singular value decomposition.

**LoRA in federated training of LLMs:** With the increasing popularity of LLMs, LoRA has been proposed to train such models in federated *cross-silo* scenarios [28, 29]. However, the main focus of existing works is fine-tuning large NN models (e.g., GPT2, LLaMA) in a communication-efficient way, still imposing large memory and computation requirements on devices. In [29], communication heterogeneity is tackled, where LoRA layers with different ranks are distributed to heterogeneous devices. Aggregation of the LoRA layers is performed similarly to HeteroFL.

*In summary, apart from recent works in fine-tuning LLMs, none of the existing works consider the availability of a set of pretrained NN models. Existing LoRA techniques [28, 29] focus on cross-silo communication and neglect memory and computation constraints in case of tiny Transformers.*

### 3 Methodology

**Problem statement:** We consider an FL (synchronous cross-device) problem, where a single *server* and many *devices*  $c \in \mathcal{C}$  exist. Training is done on the devices for several rounds  $R$ , where the server is only responsible for aggregation. Furthermore, we require that a set of pretrained tiny Transformer architectures  $\mathcal{F}$  exists, where each architecture  $F_l \in \mathcal{F}$  has a specific number of stacked layers  $l$  (specifically, a layer constitutes a multi-head attention module, as well as feedforward blocks). We assume all NNs in this set satisfy inference latency requirements. A fixed number of devices  $|\mathcal{C}^{(r)}| \ll |\mathcal{C}|$  participate every round  $r \leq R$ . Further, we assume that devices are subject to constraints. Specifically, we assume that a device can only train with a limited amount of *memory*, can be restricted in its *upload* capabilities<sup>2</sup>, and can only perform a limited number of *computations* (FLOPs) per round. Without loss of generality, we assume that these constraints are known to the server and are static over time. We label  $M_c$  as the peak memory available for training on device  $c$ . Similarly, we label  $U_c$  and  $O_c$  as the amount of upload a device can do and the computation that can be performed, respectively. Consequently, a device  $c$  can only participate in the training if the selected NN-*configuration* satisfies the given constraints.

We aim to maximize the accuracy of the FL system, given a set of devices  $\mathcal{C}$ , with a set of (heterogeneous) constraints  $\mathcal{U} = \{U_c : \forall c \in \mathcal{C}\}$ ,  $\mathcal{M} = \{M_c : \forall c \in \mathcal{C}\}$ , and  $\mathcal{O} = \{O_c : \forall c \in \mathcal{C}\}$  within a limited number of rounds  $R$ .

<sup>2</sup>We assume that only limited bandwidth is available for a device to upload its weights within a reasonable time within a round.

---

#### Algorithm 1: CAFF

---

**Input:** Total rounds  $R$ , devices  $\mathcal{C}$ , number of devices per round  $|\mathcal{C}^{(r)}|$ , device constraints  $\mathcal{M}, \mathcal{U}, \mathcal{O}$ , set of pretrained NNs

```

1:  $\mathcal{F}_{\text{feasible}} \leftarrow \{F_l \in \mathcal{F} \mid (\exists t)[t \in [1, \dots, l] \wedge \forall c \in \mathcal{C}[M_{F_l^t} \leq M_c \wedge U_{F_l^t} \leq U_c \wedge O_{F_l^t} \leq O_c]]\}$ 
2:  $\mathcal{W}^{(1)} \leftarrow \mathcal{W}_{\text{pretrained}} \leftarrow F_l // \text{ get pretrained}$ 
3: for all round  $r = 1, 2, \dots, R$  do
4:    $\mathcal{C}^{(r)} \leftarrow \text{select } |\mathcal{C}^{(r)}| \text{ devices randomly out of } \mathcal{C}$ 
5:   for device  $c \in \mathcal{C}^{(r)}$  in parallel do
6:      $\mathcal{W}^{(r)}$  receive from server
7:      $\mathcal{W}^{(r,c)} \leftarrow \text{LocalTraining}(\mathcal{W}^{(r)})$ 
8:     upload  $\mathcal{W}^{(r,c)}$ 
9:   end for
10:  for layer  $i \in [1, \dots, l]$  do
11:     $\tilde{\mathcal{W}}_i \leftarrow \bigcup_{c \in \mathcal{C}} \{W_i^{(r,c)} \mid \exists W_i^{(r,c)} \in \mathcal{W}^{(r,c)}\}$ 
12:     $W_i^{(r+1)} \leftarrow \frac{1}{|\tilde{\mathcal{W}}_i|} (\sum_{W_j \in \tilde{\mathcal{W}}_i} W_j) + (1 - \frac{1}{|\tilde{\mathcal{W}}_i|}) \cdot W_i^{(r)} // \text{ weighted averaging}$ 
13:  end for
14: end for
15:
16: LocalTraining ( $\mathcal{W}$ )
17: train  $W_i$  for  $i \in [l - t_c + 1, \dots, l]$  based on  $M_c, U_c, C_c$ 
18: Return:  $\mathcal{W} \leftarrow \{W_i \mid \forall i \in [l - t_c + 1, \dots, l]\}$ 

```

---

**Heterogeneous freezing of pretrained NNs:** We consider each NN architecture  $F_l$  to have  $l$  layers, where a specific number of these layers can be trained while others are frozen. We define  $F_l^t$  as an NN architecture with  $t \leq l$  out of a total of  $l$  layers being trained. Specifically, in  $F_l^t$ , we freeze the first  $l - t$  layers, while the remaining  $t$  layers with indices  $[l - t + 1, \dots, l]$  are being trained. Each architecture  $F_l$  can be trained with a different number of layers  $t \in [1, \dots, l]$ . We refer to  $l$  and  $t$  as a training *configuration*. Each configuration has associated resource requirements. We label  $M_{F_l^t}$  as the memory required to train  $F_l^t$ . Similarly, we label  $O_{F_l^t}$  as the computation operations (FLOPs) required, and  $U_{F_l^t}$  for communication upload, respectively. In general, a device  $c$  can only apply training to a given NN-configuration  $F_l^t$  if

$$M_{F_l^t} \leq M_c \quad \wedge \quad U_{F_l^t} \leq U_c \quad \wedge \quad O_{F_l^t} \leq O_c. \quad (1)$$

#### 3.1 NN-architecture selection with heterogeneous devices

We assume that each FL device  $c$  should be capable in participating in the training. Consequently a feasible NN structure  $F_l$  is required, where a device-specific  $t$  exists that allows all devices to apply training. Since there might be multiple architectures that allow this, we reduce the set  $\mathcal{F}$  to  $\mathcal{F}_{\text{feasible}}$  by using

$$\mathcal{F}_{\text{feasible}} \leftarrow \{F_l \in \mathcal{F} \mid (\exists t)[t \in [1, \dots, l] \wedge \forall c \in \mathcal{C}[M_{F_l^t} \leq M_c \wedge U_{F_l^t} \leq U_c \wedge O_{F_l^t} \leq O_c]]\} \quad (2)$$

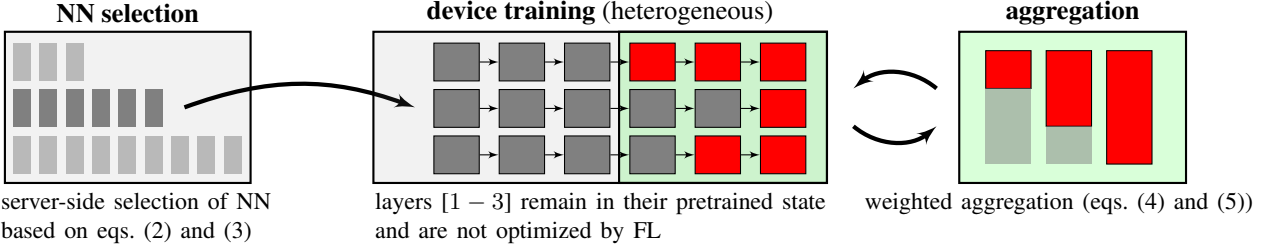


Figure 2: We propose an FL technique for cross-device FL with heterogeneous devices that incorporates the availability of pretrained models. Unlike previous approaches, our technique retains some layers in their pretrained state.

Based on our observations from preliminary experiments (such as those presented in fig. 1), we propose the following NN selection scheme. Specifically, we pick  $\hat{F}_l$  such that the average number of trained layers  $t_c$  by the devices  $c \in \mathcal{C}$  is maximized

$$\hat{F}_l = \operatorname{argmax}_{F_l} \left\{ \frac{1}{|\mathcal{C}|} \sum_{c \in \mathcal{C}} t_c \mid \forall F_l \in \mathcal{F}_{\text{feasible}} \right\}. \quad (3)$$

If there are two NNs that allow for the same average trained layers, we pick the NN with the most total layers  $l$ . This has specific implications depending on the constraint scheme. If a setting is purely peak memory or upload constrained, we observe that the associated cost of training  $t$  layers is mostly independent of the total layers  $l$  (as no activations have to be stored for frozen layers and no upload of frozen weights is required); hence, the NN with the most layers is picked. However, the number of computations (FLOPs) is impacted by  $t$  as well as by  $l$ . This is because the calculation of the frozen forward pass contributes to the computation footprint (i.e., the cost of training  $t$  layers of a 6-layered NN is lower than training  $t$  layers of a 9-layered NN). We observe (fig. 1) that, generally, training more layers of a more shallow NN maximizes the accuracy under a pure computation constraint. However, our scheme (eqs. (2) and (3)) also allow for a mixture of different constraints. We provide an ablation study for the heterogeneous case in section 4.2 to show that this strategy generally maximizes accuracy in computationally constrained cases.

We label the weights of  $F_l$  as  $\mathcal{W} = \{W_i \mid i \in [1, \dots, l]\}$ , where the weights of an individual layer are referred to as  $W_i$ . Based on its constraints, a device  $c$  selects the number of trained layers  $t_c$  and applies training to  $\mathcal{W}^{(c)} = \{W_i \mid i \in [l - t_c + 1, \dots, l]\}$ . Since layers  $[1, \dots, l - t_c]$  remain frozen, their respective parameters do not have to be uploaded to the server, saving on communication costs. On the server, we apply layer-wise weighted averaging (as done in [22]) such that for each layer  $i$ , the averaged weights  $W_i^{(r+1)}$  are determined by

$$\tilde{\mathcal{W}}_i = \bigcup_{c \in \mathcal{C}} \{W_i^{(r,c)} \mid \exists W_i^{(r,c)} \in \mathcal{W}^{(r,c)}\} \quad (4)$$

$$W_i^{(r+1)} = \frac{1}{|\tilde{\mathcal{W}}_i|} \sum_{W_j \in \tilde{\mathcal{W}}_i} W_j + (1 - \frac{1}{|\tilde{\mathcal{W}}_i|}) \cdot W_i^{(r)}, \quad (5)$$

where  $\tilde{\mathcal{W}}_i$  represents the set of weights of layer  $i$ , that are trained by the devices, and  $W_i^{(r)}$  refers to the weights of

layer  $i$  from the previous round. The NN selection and aggregation scheme is described in algorithm 1, and we provide an overview of individual components in fig. 2.

## 4 Experimental Evaluation

### 4.1 Hyperparameters and setting

**Pretraining:** We evaluate our technique and state of the art based on a set of pretrained models  $\mathcal{F}$ . Specifically, we pretrain Transformers with layers  $l \in [3, 6, 9, 12]$ . Each NN model  $F_l$  only varies in the number of layers. We use an embedding dimension of 96 and 3 heads per attention block for language modelling and 192 and 6 for ViTs. For language tasks, we use a sentencepiece tokenizer with a vocab size of 8192 and pretrain for 750K mini-batch steps on OpenWebText [14], using a context length of 256 and batch size 128. For vision tasks, we use a ViT [30] with patch size of 4 and a context length of 272. We pretrain on a down-scaled  $(3 \times 64 \times 64)$  version of ImageNet [31] for 500K steps with a batch size of 256. We apply data augmentation techniques such as random flipping, rotation, as well as random cropping. For both, vision and text domain, we use an initial learning rate of  $\eta = 5 \cdot 10^{-4}$  and use a sinusoidal decay to  $\eta = 5 \cdot 10^{-5}$  ( $1 \cdot 10^{-4}$  and  $1 \cdot 10^{-5}$  for ViT). We use AdamW [32] as optimizer ( $\beta_1 = 0.9, \beta_2 = 0.95$ ), with weight decay of 0.1 for linear layers. In all cases, dropout of 0.05 is used.

**Federated training:** We train a downstream task in a federated manner, where we distribute equal shares of Shakespeare from the Leaf benchmark [13] (next token prediction), and CIFAR10, and CIFAR100 [33] to devices  $c \in \mathcal{C}$ . Consequently, each device  $c$  has a local private dataset  $\mathcal{D}_c$ . For CIFAR and Shakespeare, we use a total of  $|\mathcal{C}| = 100$  and 10 devices per round ( $|\mathcal{C}^{(r)}| = 10$ ). We train for a total number of  $R = 75$  rounds. In the case of Shakespeare, each device randomly picks a sentence using a context length of 256 from its local text, and trains for 8 batches with batch size 32. In the case of CIFAR, each device iterates once over its data samples using batch size 32. To have the same input resolution as the data used for pretraining, we upscale CIFAR data from  $3 \times 32 \times 32$  to  $3 \times 64 \times 64$ . We distribute CIFAR100 and CIFAR10 in an non-independent and identically distributed (iid) fashion with Dirichlet  $\alpha = 0.1$  and  $\alpha = 1.0$ , respectively. We use the same optimizer setup as used in pretraining and apply learning rate decay

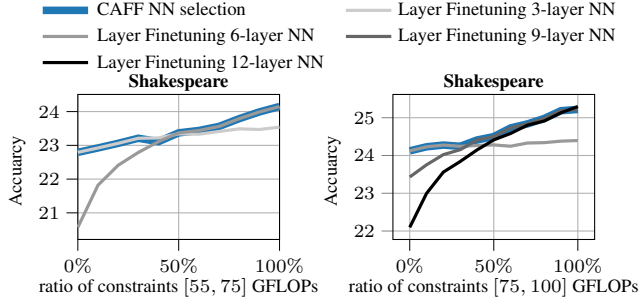


Figure 3: Ablation study of NN selection (eq. (3)). We observe that picking the NN that maximizes the average of trained layers maximizes the accuracy (blue).

from  $\eta = 1 \cdot 10^{-4}$  to  $\eta = 1 \cdot 10^{-5}$  (to  $\eta = 1 \cdot 10^{-6}$  in case of Shakespeare). In case of Shakespeare, we use weight decay of 0.1. For all federated training, dropout is set to 0. For each experiment, we report the average accuracy and standard deviation of 3 independent seeds after  $R$  total rounds of training. For CAFF, we pick the NN and number of layers to train based on eq. (2), and apply eqs. (4) and (5) for aggregation. In all cases, the Transformer’s embedding layers remain frozen, while the output layers (LayerNorm and linear layer) always receive training.

In total, we run approximately 1788 federated experiments using PyTorch 2.1 [34] using an internal cluster of NVIDIA A6000 GPUs with 50 GB of memory each (we train 894 h in total, with each experiment taking  $\sim 30$  min).

**Resource constraints:** We consider peak memory, communication, and computation as main constraints. Details about measuring a configuration’s memory, communication, and computation footprint are given details in appendix A.

## 4.2 Ablation study

To evaluate how the NN selection eq. (3) behaves when having heterogeneous devices, we mix two groups with computation constraints [55, 75] and [75, 100] GFLOPs with different rates. I.e., a rate of 10% refers to 10% of devices having a constraint of 75 while 90% have 55. For ratios between 0% and 100%, we evaluate the accuracy on Shakespeare with all feasible Transformer architectures and what  $\hat{F}_l$  is picked by our technique based on the ratio.

We can observe in fig. 3 that maximizing the average number of trained layers (as in eq. (3)) robustly picks the NN that maximizes the accuracy. Depending on the average trained layers  $t$  (which depends on the mixing ratio), eq. (3) switches from a 3 to a 6 and 6 to a 9-layered NN, maximizing the accuracy.

## 4.3 State of the art comparison

We compare CAFF against several state of the art techniques: Heterogeneous LoRA [15], FedHM [16], HeteroFL [18], FjORD [19], FedRolex [17], and DepthFL [20]. We provide details about the configuration of the state of the art in appendix B.

## 4.4 Experimental results

**Homogeneous results:** We evaluate our technique and Hetero. LoRA as well as FedHM and FedRolex in a homogeneous setting with Shakespeare and CIFAR100. Specifically, we run several experiments with homogeneous memory constraints of 500, 700, and 900 (400, 600, and 800 for ViT) MB, upload constraints of 4, 6, and 8 (8, 12, and 16 for ViT) MB, as well as computation constraints of 60, 80, and 100 (75, 150, 200 for ViT) GFLOPs. We omit results for HeteroFL, FjORD, and DepthFL, as in the homogeneous case they all degrade to vanilla FedAvg. For completeness, we visualize a range of constraints in fig. 4. To have a fair comparison, we evaluate the technique with pretrained transformers with  $l \in [3, 6, 9, 12]$  layers and present the respective highest gained accuracy in table 1. For our technique, we select the number of layers based on eq. (3).

In general, we can observe that CAFF achieves higher accuracies in almost all considered constraint settings, particularly with memory constraints. Here it can be observed that, to reach a certain accuracy, LoRA requires  $2 - 3 \times$  more memory compared to CAFF. However, LoRA achieves higher accuracies when upload constraints are applied. Additionally, it can be observed that FedRolex, when training a larger pretrained model than the devices can fully train within a round eq. (8), the accuracy heavily deteriorates. In fig. 4, we can see that with both Hetero. LoRA and FedHM lowering the rank for a specific NN impacts upload and computation but have minimal effect on the required peak memory. In contrast, CAFF supports a wider range of applicability across all three constraints.

**Heterogeneous results:** To explore how our technique performs when devices have heterogeneous constraints, we explore a scenario where 50% of devices have higher constraints than the other 50% throughout all rounds. Specifically, we evaluate a setting an equal share of devices having memory constraints of [400, 600], [600, 800], and [400, 800] ([200, 400], [400, 600], and [200, 800] for ViT) MB. Similarly, we evaluate [2, 8], [4, 8] ([2, 4] and [2, 8] MB for ViT) for upload constraints, and [55, 75] and [75, 100] ([75, 100] and [125, 200] for ViT) GFLOPs for computation, respectively.

We observe that, across most evaluated scenarios, CAFF results in higher accuracy when devices have heterogeneous constraints. For CAFF, higher average resources lead to higher final accuracy, indicating that our technique efficiently uses available resources. However, with subset-training derived techniques, this is not always the case; for instance, with higher average computation in Shakespeare, many baselines actually perform worse or do not improve. For DepthFL we observe that the additional exit of the stronger devices significantly increases the upload and memory overhead, hence, for many evaluated scenarios (especially in case of language models), no suitable configuration is available.

**Can weaker devices make a contribution to the global model?** To evaluate if weaker devices can contribute to the model, we change the data distribution from non-iid to a distribution that correlates with the devices’ constraints (similar to [22], using  $\alpha = 0.1$ ). Specifically, we distribute the data

Table 1: Accuracy for Shakespeare and CIFAR100 with homogeneous memory, upload, and computation constraints. The results show that, especially with memory constraints, CAFF (ours) outperforms the current state of the art. Only, in case of upload constraints, Heterog. LoRA shows higher effectiveness when utilizing available resources. We report – if no  $F_l$  is available.

Setting	peak memory (MB)			upload (MB)			computation (GFLOPs)		
	500	700	900	4	6	8	60	80	100
<b>Shakespeare</b>	500	700	900	4	6	8	60	80	100
CAFF (ours)	<b>23.4±0.1</b>	<b>24.9±0.3</b>	<b>25.6±0.3</b>	22.2±0.2	<b>24.8±0.2</b>	<b>25.4±0.3</b>	<b>23.1±0.1</b>	<b>24.6±0.3</b>	<b>25.0±0.2</b>
Heterog. LoRA	22.0±0.3	23.2±0.5	23.6±0.3	<b>23.2±0.2</b>	24.5±0.1	24.5±0.1	22.0±0.3	23.2±0.5	23.6±0.3
FedHM	18.5±0.3	19.0±0.2	19.0±0.2	—	—	19.0±0.2	19.0±0.2	19.0±0.2	19.0±0.2
FedRolex	1.3±0.0	4.5±0.3	4.5±0.3	3.1±0.1	4.5±0.3	4.5±0.3	4.5±0.3	4.5±0.3	4.5±0.3
<b>CIFAR100</b>	400	800	1200	8	12	16	100	150	200
CAFF (ours)	<b>56.6±0.2</b>	<b>62.2±0.5</b>	<b>63.9±0.6</b>	58.4±0.2	60.9±0.1	<b>63.7±0.4</b>	<b>43.2±1.3</b>	<b>56.1±1.2</b>	<b>60.8±1.0</b>
Heterog. LoRA	38.7±0.4	53.5±0.9	57.5±0.4	<b>62.3±0.1</b>	<b>62.3±0.1</b>	62.3±0.1	38.7±0.4	53.5±0.9	46.1±0.8
FedHM	22.7±0.4	32.0±0.6	37.3±1.3	41.0±0.2	41.0±0.2	41.0±0.2	37.3±1.3	41.0±0.2	41.0±0.2
FedRolex	1.2±0.1	1.2±0.1	1.1±0.1	1.1±0.1	1.1±0.1	1.1±0.1	1.1±0.1	1.1±0.1	1.1±0.1

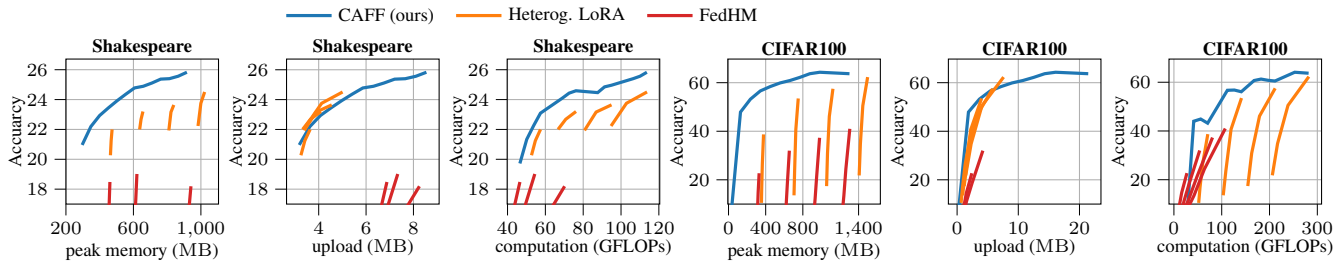


Figure 4: Visualization of homogeneous results for Shakespeare and CIFAR100. For CAFF (ours), we apply NN selection based on eqs. (2) and (3). For Heterog. LoRA and FedHM, we evaluate all NN architectures and, for a given constraint, present the best performing in table 1.

samples in CIFAR100 such that some classes are primarily available in a specific group, hence, either within the 50% of weaker or 50% of stronger devices. To evaluate how the global model performs exclusively on the weaker devices’ data, we calculate the class-specific F1-score, and weigh it with the occurrence probability of the weaker devices’ data. The results are given in table 2.

We can observe that using CAFF, the specific classes of the weaker devices are represented in the global model. However, when the variance of resources increases, weaker devices are less well represented (i.e., for memory constraints [200, 400] performs better than [200, 800] as stronger devices have more impact on the model). Contrary to that, we observe that the shared aggregation mechanism of Heterog. LoRA, FedRolex, HeteroFL, and FjORD is ineffective when such a data distribution is present, as the F1-score is 20-30 points less than when using CAFF. However, it can be seen, that in the aggregation mechanism of FedHM outperforms the other baselines. The only exception to that observation is when no suitable configuration for the baselines exists (labeled with \*, †, and ‡ in table 2), and the respective algorithms behave like in the homogeneous case (FedRolex, HeteroFL, and FjORD degrade to FedAvg in this case). For DepthFL, we see similar deterioration as in HeteroFL or FjORD. We believe this is caused by the fact that weaker devices only train the early layers instead of the last

layers and cannot sufficiently influence the stronger devices’ exit.

In summary, we find that CAFF consistently outperforms existing baselines when using pretrained tiny Transformers suitable for cross-device FL. However, in upload-constrained cases, Heterog. LoRA can outperform CAFF. When devices have heterogeneous constraints, CAFF results in higher accuracies and better resource utilization, whereas state-of-the-art methods may even see accuracy deteriorate with increased resource availability. Additionally, CAFF ensures fairer device contributions to the global model, especially when some class information is only available on weaker devices, which struggle to contribute under state-of-the-art methods.

## 5 Conclusion

In this work, we studied efficient training of pretrained tiny NNs in cross-device FL. We discovered that existing techniques like LoRA do not provide a good trade-off between resource usage and accuracy when considering peak memory and computation. Given a set of pre-trained NN architectures to choose from, we propose CAFF, an NN selection scheme and layer finetuning approach that outperforms LoRA and other state-of-the-art techniques, improving accuracy and fairness in resource-constrained scenarios. We believe that our technique, particularly the NN selection scheme, contributes to practical design considerations for

Table 2: Accuracy for Shakespeare, CIFAR10/100. To measure fairness, we evaluate the F1-score specific to the weaker devices’ data distribution. We observe that CAFF (ours) results in higher accuracies and better resource utilization, whereas state-of-the-art methods may even see accuracy deteriorate with increased resource availability.

Shakespeare	peak memory (MB)			upload (MB)		computation (GFLOPs)	
Constraint	[400,600]	[600,800]	[400,800]	[2,8]	[4,8]	[55,75]	[75,100]
CAFF (ours)	<b>23.9±0.5</b>	<b>25.1±0.4</b>	<b>24.8±0.3</b>	<b>24.6±0.4</b>	<b>25.3±0.5</b>	<b>23.3±0.4</b>	<b>24.6±0.4</b>
Heterogenous LoRA	—	21.9±0.3 <sup>‡</sup>	—	24.4±0.3	24.7±0.3	21.9±0.2	23.3±0.2
FedHM	—	18.8±0.0 <sup>†</sup>	—	—	—	18.9±0.4	19.3±0.2
FedRolex	16.2±0.2	15.7±0.1	16.2±0.2	—	16.3±0.3	16.2±0.2	15.7±0.1
HeteroFL	22.1±0.4	23.0±0.2	22.1±0.4	—	22.0±0.5	22.1±0.4	23.0±0.2
FjORD	19.8±0.3	21.5±0.1	19.8±0.3	—	19.8±0.2	19.8±0.3	21.5±0.1
DepthFL	—	—	—	—	—	—	21.7±0.4
<b>CIFAR100</b>	[200,400]	[400,600]	[200,800]	[2,4]	[2,8]	[75,100]	[125,200]
CAFF (ours)	<b>52.7±0.1</b>	<b>58.8±0.2</b>	<b>57.2±0.5</b>	<b>50.6±0.2</b>	54.1±0.4	<b>42.3±1.7</b>	<b>60.2±1.1</b>
Heterogenous LoRA	—	38.9±0.9 <sup>‡</sup>	—	45.0±1.1	<b>55.2±0.5</b>	38.9±0.9 <sup>‡</sup>	49.2±0.9
FedHM	—	23.5±1.6 <sup>†</sup>	—	—	18.0±0.6	40.1±0.6 <sup>†</sup>	31.6±1.3
FedRolex	33.9±1.0	40.7±0.8 <sup>*</sup>	33.9±1.0	—	32.7±0.6	40.7±0.8 <sup>*</sup>	44.7±2.6
HeteroFL	33.3±1.0	41.0±0.9 <sup>*</sup>	33.3±1.0	—	33.4±0.5	41.0±0.9 <sup>*</sup>	45.6±1.9
FjORD	26.3±0.3	40.1±0.9 <sup>*</sup>	26.3±0.3	—	24.2±0.5	40.1±0.9 <sup>*</sup>	37.0±1.2
DepthFL	26.8±1.2	41.0±0.9 <sup>*</sup>	26.8±1.2	—	—	41.0±0.9 <sup>*</sup>	28.7±1.3
<b>CIFAR100 (F1-score weak)</b>	[200,400]	[400,600]	[200,800]	[2,4]	[2,8]	[75,100]	[125,200]
CAFF (ours)	<b>29.8±3.4</b>	<b>49.7±2.3</b>	<b>25.9±4.3</b>	<b>36.9±2.8</b>	<b>27.4±3.3</b>	<b>46.2±1.1</b>	<b>40.4±4.6</b>
Heterogenous LoRA	—	40.2±2.9 <sup>‡</sup>	—	10.4±3.8	13.5±4.4	40.2±2.9 <sup>‡</sup>	11.8±4.0
FedHM	—	24.6±3.6 <sup>†</sup>	—	—	16.1±4.8	43.5±1.4 <sup>†</sup>	28.9±7.0
FedRolex	8.1±2.9	43.9±3.6 <sup>*</sup>	8.1±2.9	—	7.6±2.6	43.9±3.6 <sup>*</sup>	11.0±4.4
HeteroFL	8.0±2.9	43.9±3.4 <sup>*</sup>	8.0±2.9	—	7.8±2.8	43.9±3.4 <sup>*</sup>	11.0±4.6
FjORD	5.4±1.8	39.4±4.9 <sup>*</sup>	5.4±1.8	—	4.8±1.5	39.4±4.9 <sup>*</sup>	7.7±3.4
DepthFL	5.2±1.6	43.9±3.4 <sup>*</sup>	5.2±1.6	—	—	43.9±3.4 <sup>*</sup>	6.0±2.1
<b>CIFAR10</b>	[200,400]	[400,600]	[200,800]	[2,4]	[2,8]	[75,100]	[125,200]
CAFF (ours)	<b>86.9±0.1</b>	<b>89.3±0.1</b>	<b>89.8±0.1</b>	85.5±0.3	87.8±0.1	<b>82.4±0.2</b>	<b>91.1±0.2</b>
Heterogenous LoRA	—	80.1±0.1 <sup>‡</sup>	—	<b>89.4±0.6</b>	<b>90.4±0.5</b>	80.1±0.1 <sup>‡</sup>	87.3±0.5
FedHM	—	71.3±1.3 <sup>†</sup>	—	—	64.8±1.0	81.9±0.2 <sup>†</sup>	78.5±0.6
FedRolex	76.8±1.1	80.5±1.2 <sup>*</sup>	76.8±1.1	—	77.2±1.0	80.5±1.2 <sup>*</sup>	86.8±0.4
HeteroFL	76.9±1.1	80.6±1.2 <sup>*</sup>	76.9±1.1	—	77.5±1.1	80.6±1.2 <sup>*</sup>	87.1±0.3
FjORD	74.0±1.3	80.5±0.2 <sup>*</sup>	74.0±1.3	—	72.6±2.0	80.5±0.2 <sup>*</sup>	83.9±0.0
DepthFL	74.3±1.1	80.5±0.2 <sup>*</sup>	74.3±1.1	—	—	80.5±0.2 <sup>*</sup>	85.9±0.2

\* Degrades to vanilla FedAvg, † degrades to homogeneous FedHM, <sup>‡</sup> degrades to vanilla LoRA, — indicates no suitable  $F_l$ .

building efficient FL systems with device heterogeneity in mind. By leveraging pretrained models, we reduce the total resources required for training, thereby alleviating the training burden on FL devices. Moreover, our NN selection and aggregation scheme promotes higher fairness by ensuring that data from weaker devices is better represented.

## References

- [1] Zhuohan Li, Eric Wallace, Sheng Shen, Kevin Lin, Kurt Keutzer, Dan Klein, and Joey Gonzalez. “Train big, then compress: Rethinking model size for efficient training and inference of transformers”. In: *International Conference on machine learning*. PMLR. 2020, pp. 5958–5968.
- [2] Alec Radford, Jeff Wu, Rewon Child, David Luan, Dario Amodei, and Ilya Sutskever. “Language Models are Unsupervised Multitask Learners”. In: (2019).
- [3] Hugo Touvron, Thibaut Lavril, Gautier Izacard, Xavier Martinet, Marie-Anne Lachaux, Timothée Lacroix, Baptiste Rozière, Naman Goyal, Eric Ham-
- [4] Jianfeng Wang, Zhengyuan Yang, Xiaowei Hu, Linjie Li, Kevin Lin, Zhe Gan, Zicheng Liu, Ce Liu, and Lijuan Wang. “GIT: A Generative Image-to-text Transformer for Vision and Language.” In: *Trans. Mach. Learn. Res.* 2022 (2022). URL: <http://dblp.uni-trier.de/db/journals/tmlr/tmlr2022.html#WangYHLLGLLW22>.
- [5] Kilian Pfeiffer, Martin Rapp, Ramin Khalili, and Jörg Henkel. “Federated Learning for Computationally Constrained Heterogeneous Devices: A Survey”. In: *ACM Comput. Surv.* 55.14s (July 2023). ISSN: 0360-0300. DOI: 10.1145/3596907. URL: <https://doi.org/10.1145/3596907>.
- [6] Ronghang Hu and Amanpreet Singh. “Unit: Multi-modal multitask learning with a unified transformer”. In: *Proceedings of the IEEE/CVF international conference on computer vision*. 2021, pp. 1439–1449.

[7] Yiqiang Chen, Xin Qin, Jindong Wang, Chaohui Yu, and Wen Gao. “Fedhealth: A federated transfer learning framework for wearable healthcare”. In: *IEEE Intelligent Systems* 35.4 (2020), pp. 83–93.

[8] Binhang Yuan, Song Ge, and Wenhui Xing. “A federated learning framework for healthcare IoT devices”. In: *arXiv preprint arXiv:2005.05083* (2020).

[9] Bekir Sait Ciftler, Abdullatif Albaseer, Noureddine Lasla, and Mohamed Abdallah. “Federated learning for localization: A privacy-preserving crowdsourcing method”. In: *arXiv preprint arXiv:2001.01911* (2020).

[10] Jason Posner, Lewis Tseng, Moayad Aloqaily, and Yaser Jararweh. “Federated Learning in Vehicular Networks: Opportunities and Solutions”. In: *IEEE Network* (2021).

[11] Neil Houlsby, Andrei Giurgiu, Stanislaw Jastrzebski, Bruna Morrone, Quentin de Laroussilhe, Andrea Gesmundo, Mona Attariyan, and Sylvain Gelly. *Parameter-Efficient Transfer Learning for NLP*. 2019. arXiv: 1902.00751 [cs.LG].

[12] Edward J Hu, Yelong Shen, Phillip Wallis, Zeyuan Allen-Zhu, Yuanzhi Li, Shean Wang, Lu Wang, and Weizhu Chen. “Lora: Low-rank adaptation of large language models”. In: *arXiv preprint arXiv:2106.09685* (2021).

[13] S Caldas, P Wu, T Li, J Konecný, HB McMahan, V Smith, and A Talwalkar. “Leaf: A benchmark for federated settings. arXiv 2018”. In: *arXiv preprint arXiv:1812.01097* (2019).

[14] Aaron Gokaslan and Vanya Cohen. *OpenWebText Corpus*. <http://Skylion007.github.io/OpenWebTextCorpus>. 2019.

[15] Yae Jee Cho, Luyang Liu, Zheng Xu, Aldi Fahrezi, Matt Barnes, and Gauri Joshi. “Heterogeneous LoRA for Federated Fine-tuning of On-device Foundation Models”. In: *International Workshop on Federated Learning in the Age of Foundation Models in Conjunction with NeurIPS 2023*. 2023. URL: <https://openreview.net/forum?id=EmV9sGpZ7q>.

[16] Dezhong Yao, Wanning Pan, Yao Wan, Hai Jin, and Lichao Sun. “FedHM: Efficient Federated Learning for Heterogeneous Models via Low-rank Factorization”. In: *arXiv preprint arXiv:2111.14655* (2021).

[17] Samiul Alam, Luyang Liu, Ming Yan, and Mi Zhang. “FedRolex: Model-Heterogeneous Federated Learning with Rolling Sub-Model Extraction”. In: *Advances in Neural Information Processing Systems*. 2022.

[18] Enmao Diao, Jie Ding, and Vahid Tarokh. “HeteroFL: Computation and communication efficient federated learning for heterogeneous clients”. In: *International Conference on Learning Representations (ICLR)*. 2020.

[19] Samuel Horvath, Stefanos Laskaridis, Mario Almeida, Ilias Leontiadis, Stylianos I Venieris, and Nicholas D Lane. “FjORD: Fair and Accurate Federated Learning under heterogeneous targets with Ordered Dropout”. In: *arXiv preprint arXiv:2102.13451* (2021).

[20] Minjae Kim, Sangyoon Yu, Suhyun Kim, and Soo-Mook Moon. “DepthFL : Depthwise Federated Learning for Heterogeneous Clients”. In: *The Eleventh International Conference on Learning Representations*. 2023. URL: <https://openreview.net/forum?id=pf8RIZTMU58>.

[21] Sebastian Caldas, Jakub Konečný, H Brendan McMahan, and Ameet Talwalkar. “Expanding the reach of federated learning by reducing client resource requirements”. In: *arXiv preprint arXiv:1812.07210* (2018).

[22] Kilian Pfeiffer, Martin Rapp, Ramin Khalili, and Joerg Henkel. “CoCoFL: Communication- and Computation-Aware Federated Learning via Partial NN Freezing and Quantization”. In: *Transactions on Machine Learning Research* (2023). ISSN: 2835-8856. URL: <https://openreview.net/forum?id=XJlg4kQbkv>.

[23] Hui-Po Wang, Sebastian Stich, Yang He, and Mario Fritz. “ProgFed: effective, communication, and computation efficient federated learning by progressive training”. In: *International Conference on Machine Learning*. PMLR. 2022, pp. 23034–23054.

[24] Kilian Pfeiffer, Ramin Khalili, and Joerg Henkel. “Aggregating Capacity in FL through Successive Layer Training for Computationally-Constrained Devices”. In: *Thirty-seventh Conference on Neural Information Processing Systems*. 2023. URL: <https://openreview.net/forum?id=nXNsqB4Yr1>.

[25] Mehdi Setayesh, Xiaoxiao Li, and Vincent W.S. Wong. “PerFedMask: Personalized Federated Learning with Optimized Masking Vectors”. In: *The Eleventh International Conference on Learning Representations*. 2023. URL: <https://openreview.net/forum?id=hxElgUXLFF>.

[26] Erich Malan, Valentino Peluso, Andrea Calimera, Enrico Macii, and Paolo Montuschi. “Automatic Layer Freezing for Communication Efficiency in Cross-Device Federated Learning”. In: *IEEE Internet of Things Journal* (2023).

[27] Yiqun Mei, Pengfei Guo, Mo Zhou, and Vishal Patel. “Resource-Adaptive Federated Learning with All-In-One Neural Composition”. In: *Advances in Neural Information Processing Systems*. 2022.

[28] Sara Babakniya, Ahmed Elkordy, Yahya Ezzeldin, Qingfeng Liu, Kee-Bong Song, MOSTAFA EL-Khamy, and Salman Avestimehr. “SLoRA: Federated Parameter Efficient Fine-Tuning of Language Models”. In: *International Workshop on Federated Learning in the Age of Foundation Models in Conjunction with NeurIPS 2023*. 2023. URL: <https://openreview.net/forum?id=06quMTmtRV>.

[29] Fuxun Yu, Weishan Zhang, Zhuwei Qin, Zirui Xu, Di Wang, Chenchen Liu, Zhi Tian, and Xiang Chen. *Heterogeneous Federated Learning*. 2020. arXiv: 2008.06767 [cs.LG].

[30] Alexey Dosovitskiy, Lucas Beyer, Alexander Kolesnikov, Dirk Weissenborn, Xiaohua Zhai, Thomas Unterthiner, Mostafa Dehghani, Matthias Minderer, Georg Heigold, Sylvain Gelly, et al. “An image is worth 16x16 words: Transformers for image recognition at scale”. In: *arXiv preprint arXiv:2010.11929* (2020).

[31] Jia Deng, Wei Dong, Richard Socher, Li-Jia Li, Kai Li, and Li Fei-Fei. “Imagenet: A large-scale hierarchical image database”. In: *2009 IEEE conference on computer vision and pattern recognition*. Ieee. 2009, pp. 248–255.

[32] Ilya Loshchilov and Frank Hutter. “Decoupled weight decay regularization”. In: *arXiv preprint arXiv:1711.05101* (2017).

[33] Alex Krizhevsky, Geoffrey Hinton, et al. *Learning multiple layers of features from tiny images*. 2009.

[34] Adam Paszke, Sam Gross, Francisco Massa, Adam Lerer, James Bradbury, Gregory Chanan, Trevor Killeen, Zeming Lin, Natalia Gimelshein, Luca Antiga, Alban Desmaison, Andreas Kopf, Edward Yang, Zachary DeVito, Martin Raison, Alykhan Tejani, Sasank Chilamkurthy, Benoit Steiner, Lu Fang, Junjie Bai, and Soumith Chintala. “PyTorch: An Imperative Style, High-Performance Deep Learning Library”. In: *Advances in Neural Information Processing Systems 32*. Ed. by H. Wallach, H. Larochelle, A. Beygelzimer, F. d’Alché-Buc, E. Fox, and R. Garnett. Curran Associates, Inc., 2019, pp. 8024–8035. URL: <http://papers.neurips.cc/paper/9015-pytorch-an-imperative-style-high-performance-deep-learning-library.pdf>.

## A Technical details of constraint evaluation

**Peak Memory:** Peak memory is measured by summing the three major components that impact peak memory: the number of weights that must be kept in memory, the optimizer state of AdamW, and the activations that must be stored in memory. Activations that must be kept in memory are collected by traversing the compute graph during backpropagation in PyTorch [34].

**Communication:** The amount of data (in MB) that needs to be uploaded by a device is computed by tracking the parameters that change during training on the device (i.e., unfrozen parameters). Unchanged parameters do not need to be uploaded.

**Computation:** The number of GFLOPs required for a single mini-batch during training is calculated by determining the forward and backward operations needed for major operations such as linear layers, dot products, addition, and layer normalization.

### A.1 Training memory components

We analyze the different memory components involved in training with layer freezing as used in CAFF and baselines. The components *parameters*, *gradients and optimizer states*, and *activations* are visualized for layer freezing and LoRA in fig. 5. It can be observed that LoRA consistently requires

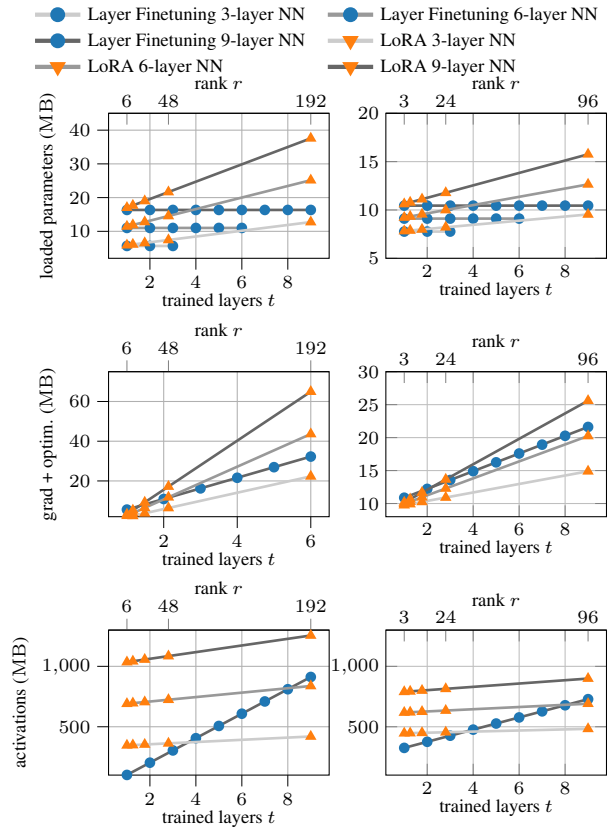


Figure 5: Memory components of layer fintuning and LoRA for language models (right) and ViTs (left) with 3, 6, and 9 layers.

more memory for loaded parameters compared to layer finetuning, due to the additional low-rank adapters. Conversely, LoRA demands less memory for gradients and optimizer states. However, activation memory constitutes the majority of the overall memory footprint for the evaluated transformer sizes. In this context, LoRA does not reduce activation memory since activations must be stored in memory for backpropagation, even when the main parameters of the transformer are frozen.

In contrast, with layer finetuning, the memory required for activations, gradients, and optimizer states is independent of the total number of layers and decreases linearly with the number of frozen layers. LoRA is very effective when gradients dominate the memory footprint. For large models (i.e., those with a large embedding dimension), this is the case, as gradients grow quadratically with the embedding dimension, while the activations only linearly depend on the embedding dimension.

## B State of the art comparison

**Heterogeneous LoRA [15]:** LoRA applies a low-rank adapter to linear operations in the NN’s layers. To support heterogeneity, the low-rank adapters are aggregated similarly to HeteroFL [18]. We freeze the token and position embedding table similar to layer finetuning. All LayerNorm modules receive training. We fully train the output linear layer as we have seen bad performance when using low-rank adapters.

**FedHM [16]:** In FedHM, a lower complexity model is created by applying a singular value decomposition (SVD) to linear layers  $w \in \mathbb{R}^{P \times Q}$  such that  $U, S, V^T = \text{svd}(w)$ . Using a lower rank  $z$ , an approximation of  $w \sim U \cdot \text{diag}(S) \cdot V^T$  can be constructed using two consecutive linear layers with  $U \cdot \text{diag}(S) \in \mathbb{R}^{P \times z}$  and  $V^T \in \mathbb{R}^{z \times Q}$ . We pick the NN structure so that the least constrained device can fully train the NN without using SVD. All devices with less resources pick  $z$  s.t.

$$z_s = \max(z) \quad \text{s.t.} \quad M_{F^z} \leq M_c \wedge U_{F^z} \leq U_c \wedge O_{F^z} \leq O_c. \quad (6)$$

The parameters  $w$  are reconstructed on the server for aggregation by using  $U \cdot \text{diag}(S) \cdot V^T$ .

**HeteroFL: [18]:** HeteroFL is a state-of-the-art technique that enables heterogeneous devices to train a common NN model. This is achieved by training a subset of the full NN architecture. Let  $w \in \mathbb{R}^{P \times Q}$  represent a linear layer in a Transformer NN. To lower the resources, constrained devices scale down the NN by using a subset of  $w$  using a scale factor  $s \in (0, 1]$ , such that  $\tilde{w} \in \mathbb{R}^{\lfloor sP \rfloor \times \lfloor sQ \rfloor}$ . Scaling down linear layers with  $s$  results in a quadratic reduction in parameters (hence upload and computation), but only in a linear reduction in memory (as activations make up for most required memory, which decreases linearly with  $s$ ). In HeteroFL, constrained devices receive always the same fixed subset of the full weights  $w$ . We introduce  $I$  as the set of indices, that are used to create a subset. In HeteroFL, a device  $c$  with a constraint  $s$  uses a subset of size  $\lfloor sP \rfloor \times \lfloor sQ \rfloor$  by using  $I_Q \in \{i | 0 \leq i < \lfloor sQ \rfloor - 1\}$  as output indices and  $I_P \in \{i | 0 \leq i < \lfloor sP \rfloor - 1\}$  as input indices. HeteroFL

requires that a share of FL devices are capable of training the full NN weights. Therefore, we select the NN structure with the most layers that can still be fully trained ( $s = 1$ ) by a single participating device. Remaining devices create a submodel  $\hat{F}^s$  that supports their constraint by using

$$s_c = \max(s) \quad \text{s.t.} \quad M_{\hat{F}^s} \leq M_c \wedge U_{\hat{F}^s} \leq U_c \wedge O_{\hat{F}^s} \leq O_c. \quad (7)$$

**FjORD [19]:** FjORD applies the same strategy as HeteroFL with respect to indices. However, a constrained device switches on a mini-batch level between different levels of  $s$ .

**FedRolex [17]:** Here, devices use a subset similarly to HeteroFL. However, while in HeteroFL, a constrained device always trains the same slice of weights  $w$ , in FedRolex, a rolling window approach is used. Output indices are selected per round  $r$ , such that for a linear layer  $w$ ,  $I$  is selected using

$$I^{(r)} = \{\hat{r}, \hat{r} + 1, \dots, r + \lfloor s_c Q \rfloor - 1\} \quad (8)$$

in case  $\hat{r} + \lfloor s_c Q \rfloor \leq Q$ .

$$\{\hat{r}, \hat{r} + 1, \dots, Q - 1\} \cup \{0, \dots, \hat{r} + \lfloor s_c Q \rfloor - 1 - Q\} \quad (9)$$

otherwise, where  $\hat{r} = r \bmod Q$ . Thereby, FedRolex eventually trains all weights of an NN, even if no device can fully train all parameters within a round.

**DepthFL [20]:** As we evaluate devices within two distinct resource groups, we configure DepthFL such that the weaker devices use a single early exit, while the stronger devices use the same early exit as the weaker devices, as well as the last exit of the NN structure. On the server, we evaluate the accuracy based on the last exit of the NN.